مجلة الدراسات التربوية والعلمية - كلية التربية - الجامعة العراقية
العدد السادس والعشرون - المجلد الأول - علوم الفيزياء - أيلول 2025 م
doi.org/10.52866/esj.2025.01.26.21

Effect of Nano-ZrO_2 Reinforcement on the Physical, Thermal, and Electrical Properties of Aluminum 7075 Alloy

Alaa Hussein Ali[1] , Faris Salih Alatallah[2] , Yahya Abdulkareem Salman[3]
Deparment of Physics/ College of Science/ Tikrit University[1,2],
Deparment of Physics/ College of Science/ Mosul University, Iraq.[3]
alla.h.ali@st.tu.edu.iq[1] , f-s.atallah@tu.edu.iq[2] , Yahya200138@uomosul.edu.iq[3].
Corresponding author: Alaa Hussein Ali, alla.h.ali@st.tu.edu.iq

Abstract:

The research deals with improving the thermal, electrical, and physical properties of 7075 aluminum alloy using nano zirconium oxide (ZrO_2) as reinforcement. The composite materials were prepared using the powder metallurgy technique to achieve a homogeneous distribution of the reinforcement particles. The effect of different percentages of ZrO_2 (0.5%, 1%, 1.5%, and 2%) on the alloy was studied. The study included physical tests (density, porosity), structural analyses (XRD, SEM), as well heat conversion and electrical properties. The results XRD showed the peaks in the Al7075/ZrO_2 composite are shifted to a lower 2θ. it proved the SEM, that the ZrO_2 reinforcement particles were evenly distributed. The apparent density increased from 4.7 to 5.4 g/cm^3, while the bulk density increased from 2.8 to 3.8g/cm^3, the apparent porosity decreased from 39 to 16%, while the true porosity decreased from 33 to 14 %. The thermal conductivity decreased from 130 w/m. k to 109 w/m. k, and the electrical conductivity decreased from 25x10^6 s/m to 20x10^6 s/m. with increasing ZrO_2 content.

Keywords: Al7075 alloy, Nano ZrO_2, Powder metallurgy, Thermal properties, Electrical conductivity, Porosity, density.

تأثير التدعيم باستخدام أكسيد الزركونيوم النانوي على الخواص الفيزيائية والحرارية والكهربائية لسبائك الألومنيوم 7075

علاء حسين علي[1] ، فارس صالح عطاالله[2] ، يحيى عبدالكريم سلمان[3]
[1,2] قسم الفيزياء، كلية العلوم، جامعة تكريت، العراق.
[3] قسم الفيزياء، كلية العلوم، جامعة الموصل، العراق.

مستخلص:

يتناول البحث تحسين الخصائص الحرارية والكهربائية والفيزيائية لسبائك الألومنيوم 7075 باستخدام أكسيد الزركونيوم النانوي (ZrO2) كتدعيم. تم تحضير المواد المركبة باستخدام تقنية مسحوق المعادن لتحقيق توزيع متجانس لجزيئات التدعيم. تمت دراسة تأثير النسب المئوية المختلفة من ZrO_2 (0.5٪، 1٪، 1.5٪، و 2٪) على السبيكة. تضمنت الدراسة الاختبارات الفيزيائية (الكثافة، المسامية)، والتحليلات البنيوية (XRD، SEM)، وكذلك التحويل الحراري والخصائص الكهربائية. أظهرت نتائج XRD أن القمم في المركب Al7075 / ZrO2 قد تحولت إلى θ2 أقل. أثبت فحص المجهر الالكتروني الماسح، أن جزيئات التدعيم ZrO_2 موزعة بالتساوي. زادت الكثافة الظاهرية من 4.7 إلى 5.4 g/cm^3، بينما زادت الكثافة الظاهرية من 2.8 إلى 3.8g/cm^3، انخفضت المسامية الظاهرية من 39 إلى 16٪، بينما انخفضت المسامية الحقيقية من 33 إلى 14٪. وانخفضت الموصلية الحرارية من 130 إلى w/m.k109، وانخفضت الموصلية الكهربائية من 25*10^6 إلى s/m20*10^6 مع زيادة محتوى أكسيد الزركونيوم.

الكلمات المفتاحية: سبائك7075، أكسيد الزركونيوم النانوي، ميتالورجيا المساحيق، الخواص الحرارية، التوصيل الكهربائي، المسامية، الكثافة.

1. Introduction

Aluminum 7075 is a widely used aerospace-grade alloy, celebrated for its high strength-to-weight ratio, excellent fatigue resistance, and machinability. Despite its superior mechanical properties, certain applications demand further enhancements in thermal stability, electrical conductivity, and physical characteristics. This has driven the exploration of advanced composite materials reinforced with nanoscale ceramics, such as nano-zirconium oxide (ZrO_2) [1].

Nano-ZrO_2 is renowned for its remarkable thermal stability, corrosion resistance, and mechanical robustness. When integrated into metal matrices like Aluminum 7075, it can significantly enhance the material's performance, addressing limitations in extreme operating environments. For instance, the thermal properties of ZrO_2 contribute to improved heat dissipation, while its structural reinforcement enhances wear resistance and overall mechanical stability. Additionally, the electrical properties of the composite can be fine-tuned, potentially broadening its application in advanced electronic and aerospace systems [2].

Research in this area highlights the synergistic effects of nano-ZrO_2 inclusions on aluminum alloys, revealing promising improvements in hardness, tensile strength, and thermal conductivity. Such advancements underscore the potential of nano-ZrO_2-reinforced composites in critical sectors, including aerospace, automotive, and energy industries. This study aims to explore these enhancements in detail, contributing to the growing body of knowledge on nanocomposite materials [3].

Powder metallurgy (PM) has emerged as a leading manufacturing technique for these composites due to its ability to produce uniform dispersions of reinforcement particles. This process involves mixing aluminum powder with nano-ZrO_2 particles, followed by compaction and sintering under controlled conditions. Powder metallurgy allows precise control over particle distribution and density, which are critical for achieving optimal material properties. Additionally, it minimizes material wastage and allows for the production of complex shapes with tailored properties. Studies have demonstrated that composites produced via PM exhibit superior mechanical and thermal characteristics compared to those manufactured using conventional methods. This makes PM an attractive choice for the industrial-scale production of nano-ZrO_2-reinforced Aluminum 7075 composites [4, 5, 6].

This study is to investigate the effects of nano-ZrO_2 reinforcement on the thermal, electrical, and physical properties of Aluminum 7075 composites. This research seeks to establish a comprehensive understanding of the material behavior, thereby offering insights into the optimization of manufacturing processes. Ultimately, this work aspires to contribute to the development of high-performance composites for applications in aerospace, automotive, and other high-demand sectors.

2. Experimental study

Raw Materials (Powders) Used:

The powders were utilized in the preparation of the composite material, with aluminum alloy (AL7075) serving as the matrix material. Table (1) presents the specifications of the powders used, including their purity, particle size, origin, density, and proportions. The reinforcement material is the nano-oxide: zirconia (ZrO_2), Table (2) provides the specifications of the nano-oxide powder as well.

Table (1): Specifications of Powders for Aluminum Alloy (Al7075) Prepared Using Powder Metallurgy

Powder Type	Purity (%)	Particle Size (nm)	Origin	Density (g/cm³)	Proportion (%)
Aluminum (Al)	99.5	≥63	Indian	2.81	90
Zinc (Zn)	99.5	≥63	Indian	7.14	5.67
Magnesium (Mg)	99.5	≥63	Indian	1.74	2.5
Copper (Cu)	99.5	≥63	Indian	8.96	1.6
Chromium (Cr)	99.5	≥63	Indian	7.19	0.23

Table (2): Specifications of Nano-Oxide Powders of American Origin

Powder Type	Purity (%)	Particle Size (nm)	Origin	Density (g/cm³)
Nano Zirconium Oxide (ZrO_2)	100	≥50	American	5.89

Powers Mixing

The powders were mixed thoroughly in a steel container and steel balls with a diameter of (10 mm) were placed and formed with a homemade electric mixer. The powders were mixed in the proportions given in Table (1) to prepare the aluminum alloy (AL7075). The reinforcement powders were also mixed and blended by adding different weight proportions of nano oxides with the base material (AL7075) as in Table (3) and were mixed well to obtain a homogeneous mixture.

Table (3): The weight percentages for each composite

		Al7075	**A1**	**A2**	**A3**	**A4**
Composite	**Al 7075**	**100**	**99.5**	**99**	**98.5**	**98**
	ZrO2	0	0.5	1	1.5	2

Powder Pressing

After weighing the materials and mixing them accurately to obtain a homogeneous powder, the samples were pressed and formed using the Unixaxil pressing method using a steel mold made of steel with a diameter of (10mm). After that, the well-mixed powder was placed inside the mold and the mold was placed inside the German-made hydraulic press of the type (DK 7510 BARRIT DENMARK) with a pressing capacity of (40Ton) and a load of (8Ton) was applied for (30 Sec), to ensure that elastic return does not occur, and to obtain cylindrical samples with a diameter of (10mm).

Figure 1: The samples obtained after pressing the powders

Sintering

The thermal sintering process was carried out using a German-made (QUAYLE DENTAL) electric furnace that reaches a temperature of (900°C). A (65cm) long tube made of heat-resistant stainless steel was used, open at one end and closed at the other end with a plug of thermal clay. It was connected to an electric discharge device (Rotary Pump) that was used to obtain a high discharge to prevent oxidation of the samples during the thermal sintering process. The furnace temperature was raised to (500°C), which is the sintering temperature, while the samples were kept inside the furnace for an hour and a half, then the furnace was turned off, and the samples were kept inside the furnace until the next day until the samples cooled slowly inside the furnace to room temperature.

3. Examinations and Testing

Structural characterization

After sintering, the samples were smoothed and polished using polishing papers with grit sizes ranging from 2000 to 4000 to achieve a fine surface finish. The microstructural characterization of the samples was performed by performing XRD and FESEM analyses. Characterization. The XRD analysis of the samples was performed using X-ray diffraction testing was conducted using a device of type (x'Peart Highscore Plus) of Dutch origin. with a scan rate of 4°/min and a step size of 0.02° with CuKα radiation (λ = 1.5405 Å). The morphology of the samples was analyzed by FESEM Type (TESCAN), Model (MIRA3), and French origin.

Physical Tests

Physical assessments were performed, encompassing apparent and volumetric density, apparent and real porosity, in addition to water absorption. The tests were performed utilizing the Archimedes principle approach in accordance with the international standard (ASTM C373-88) [7]. An accurate German-made electric balance with a precision of (0.0001g) was employed, following these steps: -

1- The samples were subjected to drying for one hour in an electric oven at a temperature of 100°C, remaining in the oven until they cooled. Upon extraction from the oven, the samples were weighed to determine the dry weight (Wd).

2- The samples were submerged for

24 hours in a vessel containing distilled water at ambient temperature. The samples were subsequently extracted from the water, and only the water droplets adhering to the surface of the samples were eliminated. The samples were subsequently weighed to determine the saturated weight (Ws).

3- The materials were weighed in distilled water using a precise suspension balance to determine the suspended weight (W_i).

In order to determine water absorption, apparent porosity, bulk density, saturated weight, and dry weight, one must first know the three weights. The following relationships are used to calculate them:

$$T.D = \sum_{i=1}^{n}(\rho_i . X_i) \quad .... (1)$$

Where: T.D: theoretical density, ρ_i: theoretical density of the elements composing the single body (g/cm3), X_i: percentage of each element in the body.

$$\rho_a = \left(\frac{W_d}{W_d - W_i}\right) * \rho_w \quad .... (2)$$

Where: ρ_a: Apparent Density (g/cm3), ρ_w: Density of water (g/cm3), W_d = dry weight of the body (g), W_i = weight of the body suspended in water (g).

$$\rho_b = (W_D/(W_s - W_i)))*\rho_w \quad ....3$$

Where: ρ_b: bulk density (gm/cm3), W_s: weight of the body saturated with water (g).

$$A.P. = \frac{W_s - W_d}{W_s - W_i} * 100\% \quad ....4$$

Where: A.P: Apparent Porosity

$$T.P. = \frac{T.D. - B.D.}{T.D.} * 100\% \quad .... (5)$$

Where: T.P.: Total porosity ratio of the sintered body, T.D.: theoretical density of the sintered body (gm/cm3).

$$W.A = W_s - \frac{W_d}{W_d} * 100\% \quad .... (6)$$

Where: W.A: Water Absorption Capacity.

Electrical Conductivity Test

The electrical conductivity test was performed using an American-made LCR-Meter, type (Precision Impedance, Analyzer Agilent 4294A, USA). The electrical conductivity was calculated from the following relationship, and the electrical resistance was calculated from the reciprocal of the electrical conductivity.

$$\sigma_{A.C} = 2\pi f \varepsilon_\circ \varepsilon'' \quad .... (7)$$

Where: $\varepsilon_\circ$ is the permittivity of vacuum and its value is 8.854×10^{-12} F/m, f Frequency in HZ for each sample

$$\rho_{a.c} = \frac{1}{\sigma_{a.c}} \quad .... (8)$$

Thermal Conductivity Test

The thermal conductivity test was conducted using a Heat conversion unit manufactured by P.A. Hilton Ltd England. The thermal conductivity coefficient (K) is calculated from the Fourier Law equation:

$$-k = \frac{Q}{A \times \frac{\Delta T}{\Delta X}} \quad .... (9)$$

Where: k: Thermal conductivity coefficient (w/m.k), Q: The amount of heat passing through per unit time (w), A: Cross-sectional area of heat flow (m^2), $\Delta T/\Delta X$: Thermal gradient with respect to distance (k/m).

4. Results and discussion

Microstructural analysis

X-Ray diffraction of Al7075/ZrO2 composites

Reinforced Al7075 with ZrO_2 particles at varying percentages (0.5, 1, 1.5, and 2%), the XRD pattern of the resulting Al7075/ZrO_2 composite is displayed in Figure 3. Zirconia and aluminum peaks can be seen in the XRD pattern. which peaks grows as the weight fraction of ZrO_2 particles increases. In contrast to the Al7075 material, the Al7075 peaks in the Al7075/ZrO_2 composite are somewhat shifted to a lower 2θ. The stability of the Al7075/ZrO_2 composite is demonstrated by the XRD pattern. Adding ZrO_2 particles to Al7075 material does not result in the production of intermetallic compounds. The XRD pattern further proves that the ZrO_2 and Al7075 matrix materials are pure. As well as this aligns with [8].

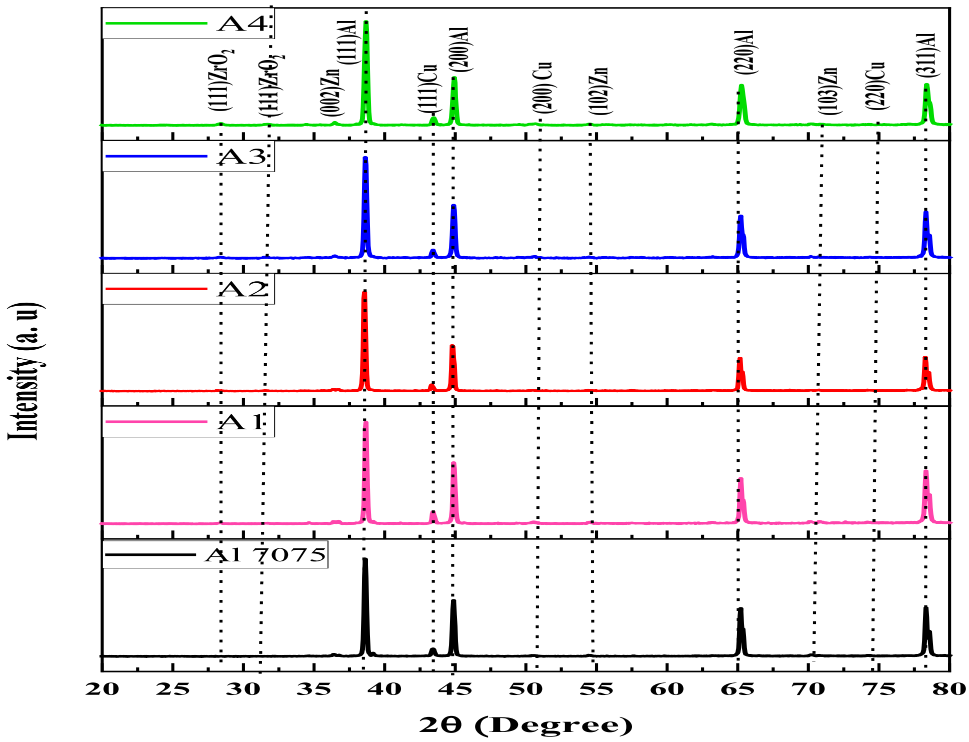

Figure 2: X-ray diffraction of Al7075 alloys the reinforcement with different proportions of ZrO_2.

SEM and EDX analysis

Composites with ZrO_2 (0.5, 1, 1.5, and 2 wt.%) reinforced particles and pure Al7075 are shown in SEM micrographs in Figure 3(a) and (b). It seems that the ZrO_2 particles in the Al7075 material have a spherical shape, as seen in the figure. Adding ZrO_2 particles to the composite causes the reinforcement particles to disperse evenly along the grain boundaries, as shown in the SEM micrographs. Additionally, it proved that the ZrO_2 reinforcement particles were evenly distributed, which decreased the likelihood of particle aggregation. The synthesis of composites, which involves powder milling, is responsible for this achievement [9]. Porosity in the Al7075/ZrO_2 composite is decreased due to the reduction of agglomeration and segregation, which is achieved by improving the uniform distribution of ZrO_2 reinforcement particles. As a result, the composites' mechanical behavior is enhanced [10]. In Figure 3(b), we can observe the composite Al7075/ZrO_2 energy-dispersive spectra. The presence of aluminum, Zr, and O is demonstrated by the peaks, according to the EDS studies. As a result, we know that the composite contains ZrO_2 particles. The composition of the Al7075/ZrO_2 composite sample can be better understood with the use of this study.

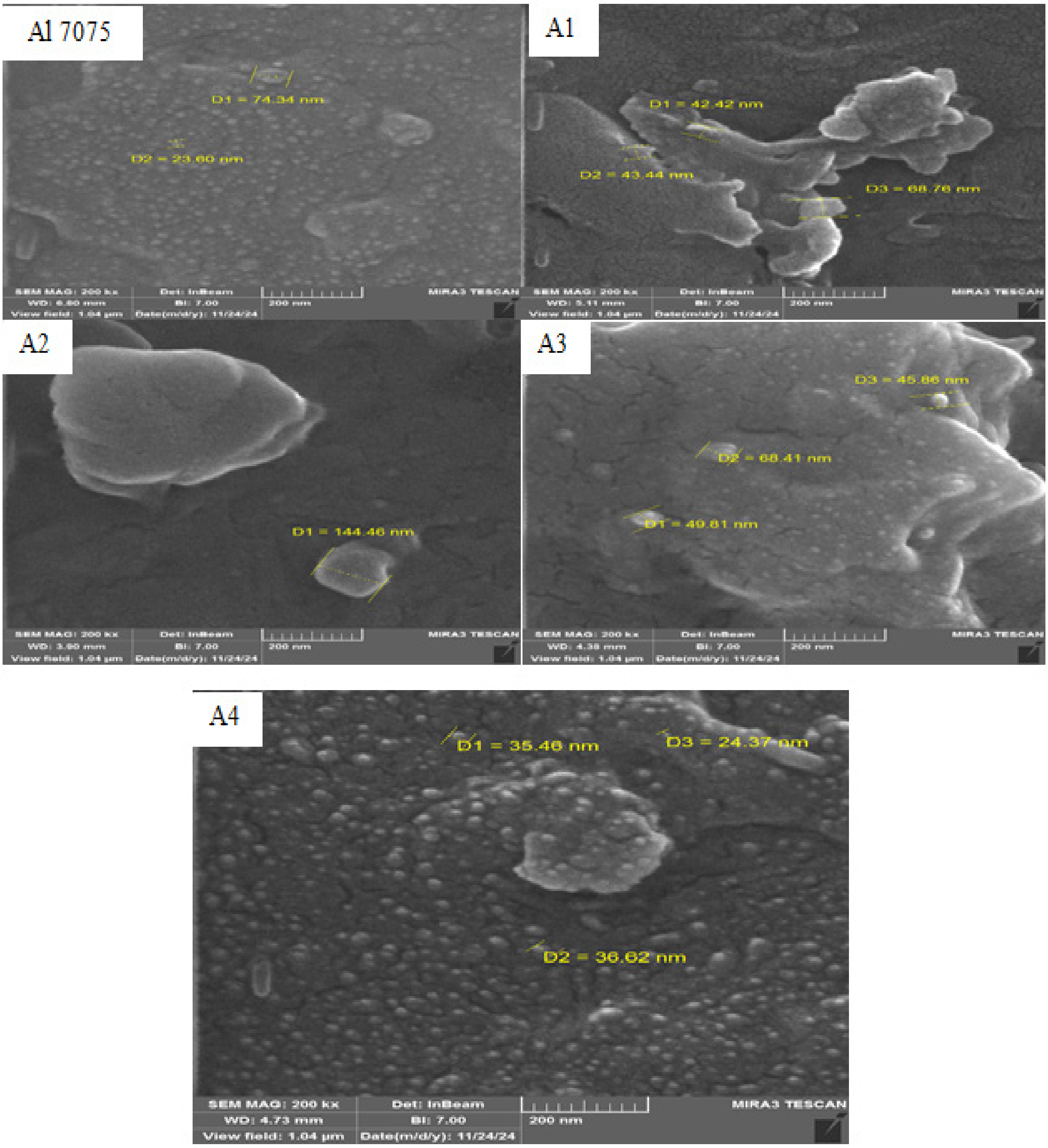

Figure 3 (a): show effect ZrO_2 content on SEM analysis of Al7075 alloys.

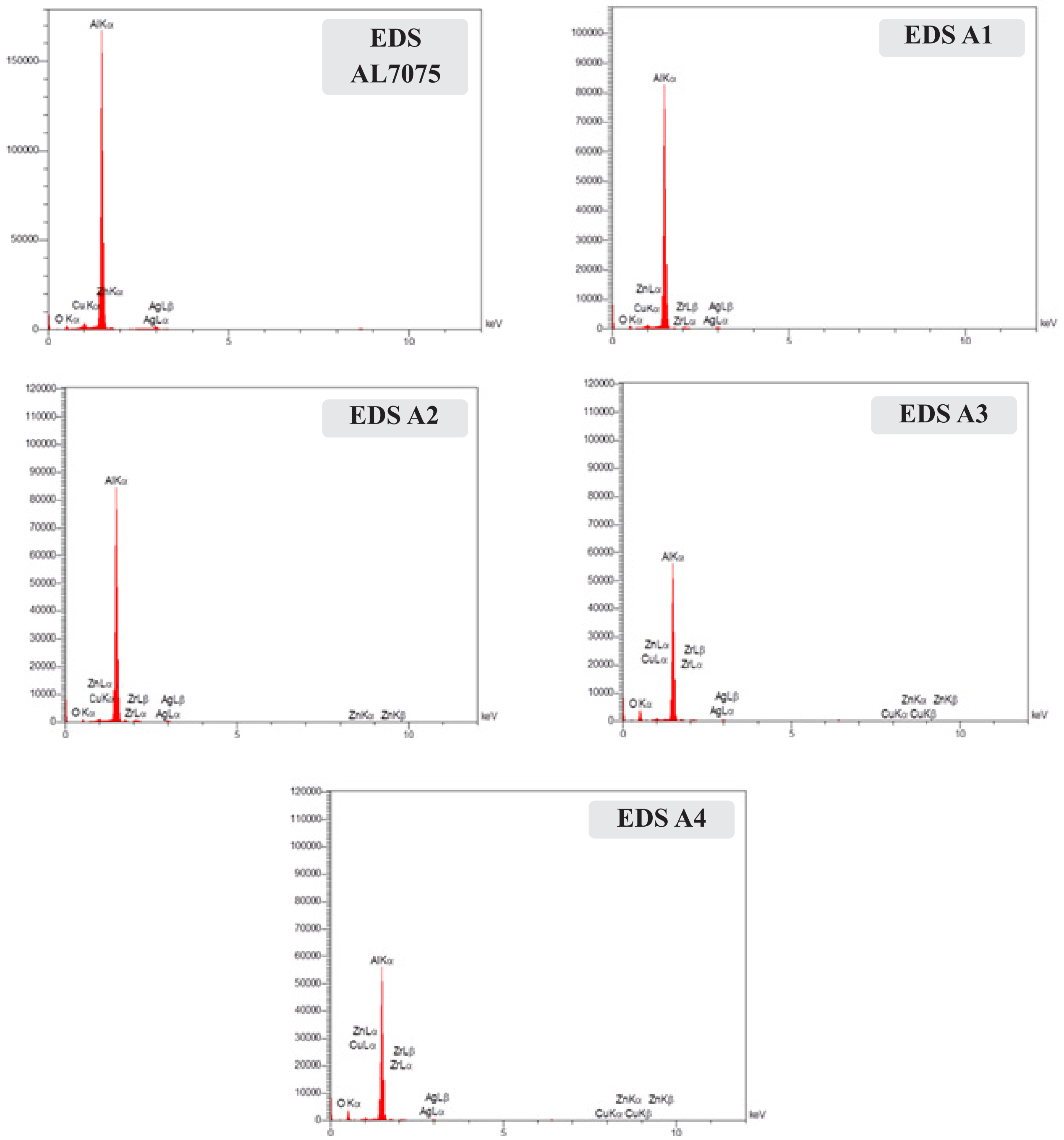

Figure 3 (b): show effect ZrO$_2$ content on EDS analysis of Al7075 alloys.

Physical properties:

Figure (4), shows the effect of adding zirconium dioxide (ZrO_2) on the apparent density and bulk density of Al7075 aluminum alloy. The figure shows that increasing the ZrO_2 content leads to an increase in density. When

ZrO_2 is added in small amounts, it acts as a binding agent that improves the cohesion between the grains, which leads to a reduction in voids. At addition ratios (0.5%-1.5%), there a limited effect because the material has reached a metastable state where the structural effects begin to saturate. At higher ratios (1.5%-2%), the ZrO_2 particles are more uniformly distributed and the microstructure of the alloy is rearranged, improving the structural cohesion and hardness due to the enhanced interpenetration between the grains, which leads to a significant increase in density. The addition of ZrO_2 improves the order of the crystal lattice and reduces crystal defects (such as voids between particles) as a stabilizing agent, which leads to reduced porosity and increased density. In addition, ZrO_2 has a higher density than aluminum ($ZrO_2 \approx 5.68$ g/cm³ compared to Al ≈ 2.7 g/cm³), and thus its incorporation leads to an increase in the density of the alloy, and this agrees with [11, 12].

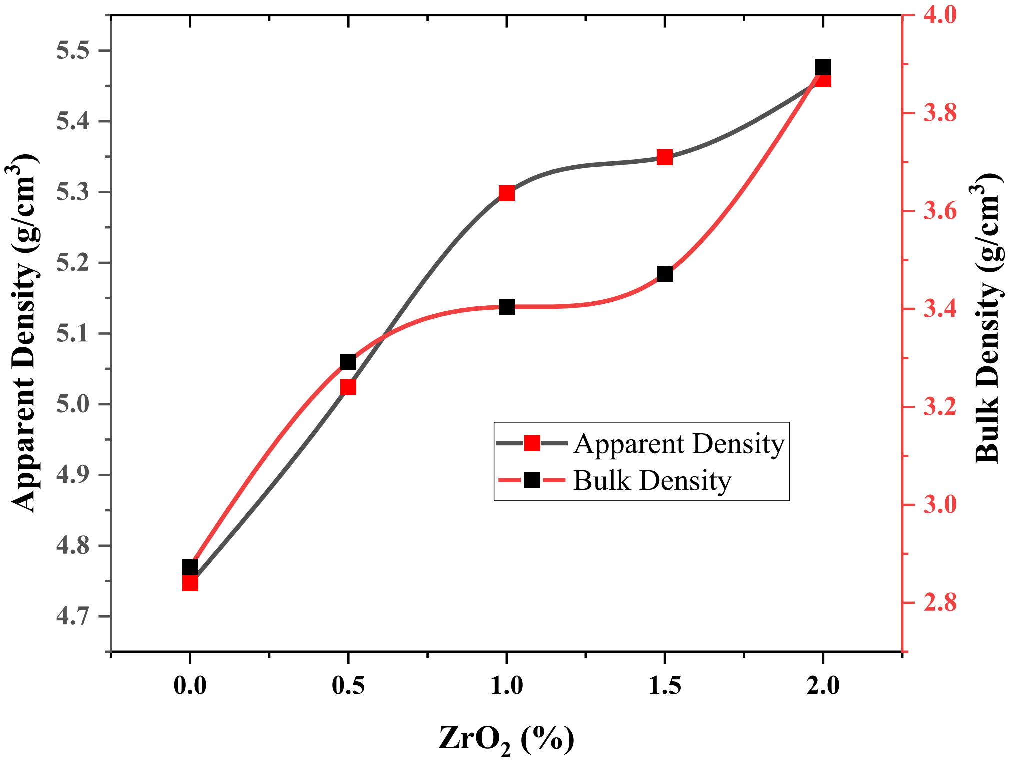

Figure 4: shows the effect of ZrO_2 content on Apparent and Bulk density for Al7075 Alloy.

Apparent and True Porosity

Figure (5) shows the effect of adding zirconia (ZrO_2) on both the apparent porosity and true porosity of Al7075 aluminum alloy. It is shown that the apparent porosity decreases with increasing zirconia content. At zirconia content (0%), the apparent porosity is about 40%. With increasing zirconia content to 2%, the apparent porosity decreases to about 15%. This is attributed to the fact that adding zirconia improves the alloy structure by reducing the apparent porosity. The figure shows a similar decrease in true porosity with increasing zirconia content. The true porosity starts at about 35% at zirconia content (0%) and reaches about 10% at zirconia content (2%). This shows that the effect of zirconia extends to improving the material density and particle distribution within the alloy. And this agrees with [13, 14].

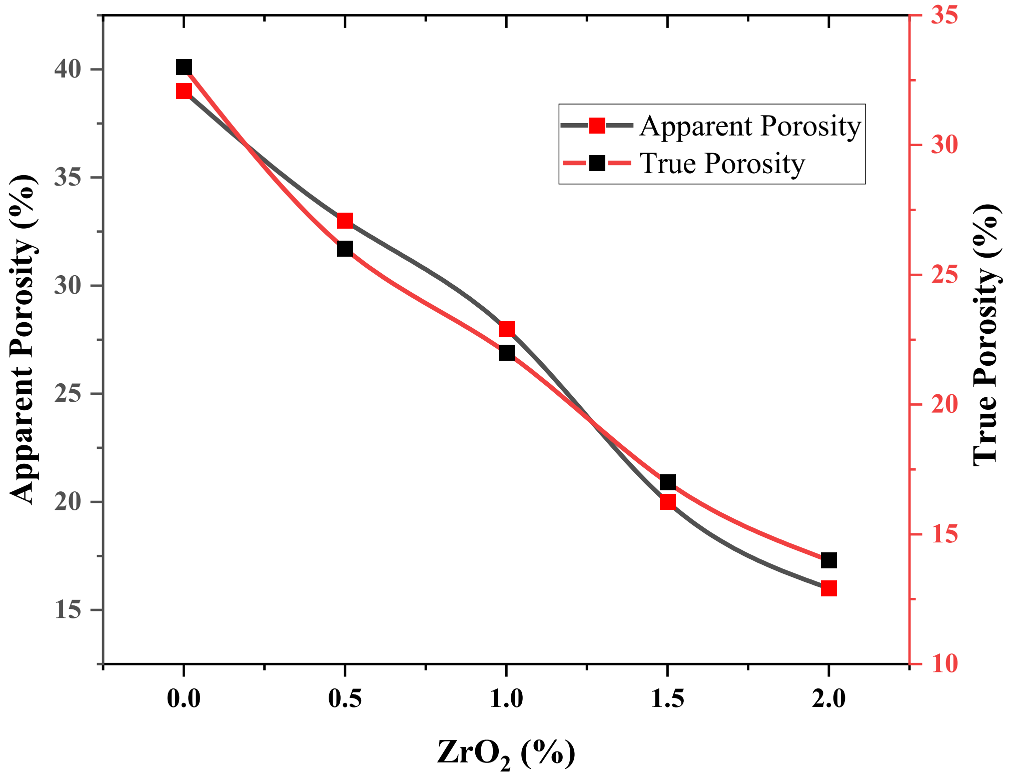

Figure 5: show the effect of ZrO_2 content on Apparent and True porosity for Al7075 Alloy.

Electrical and thermal properties

Figure (6a, b) shows the relationship between the percentage of adding (ZrO_2) to the Al7075 alloy and the thermal, and electrical conductivity of the alloy.

Figure (6, a) shows the decrease in the thermal conductivity of the alloy with the increase in the percentage of zirconium oxide. The conductivity decreased from (130 w/m.k) for the pure alloy to (109.2 w/m.k) at (2%) zirconium oxide. This decrease is attributed to the fact that zirconium oxide contributes to changing the microstructure of the alloy as zirconium oxide is distributed in the form of particles in the alloy, which hinders the movement of electrons and phonons. With the increase in the zirconium oxide content, the thermally insulating regions in the material increase, which reduces the overall thermal conductivity of the alloy which agrees with [11].

Figure (6, b) shows the decrease in electrical conductivity with increasing zirconium oxide content in the aluminum alloy from (250x105 s/m) for the pure alloy to (20x105 s/m) at a content of (2%) zirconia oxide. This decrease is attributed to the fact that zirconium oxide particles act as impurities or dispersants within the crystal structure. They hinder the movement of free electrons. The electronic dispersion increases at the crystal boundaries. This agrees with [15].

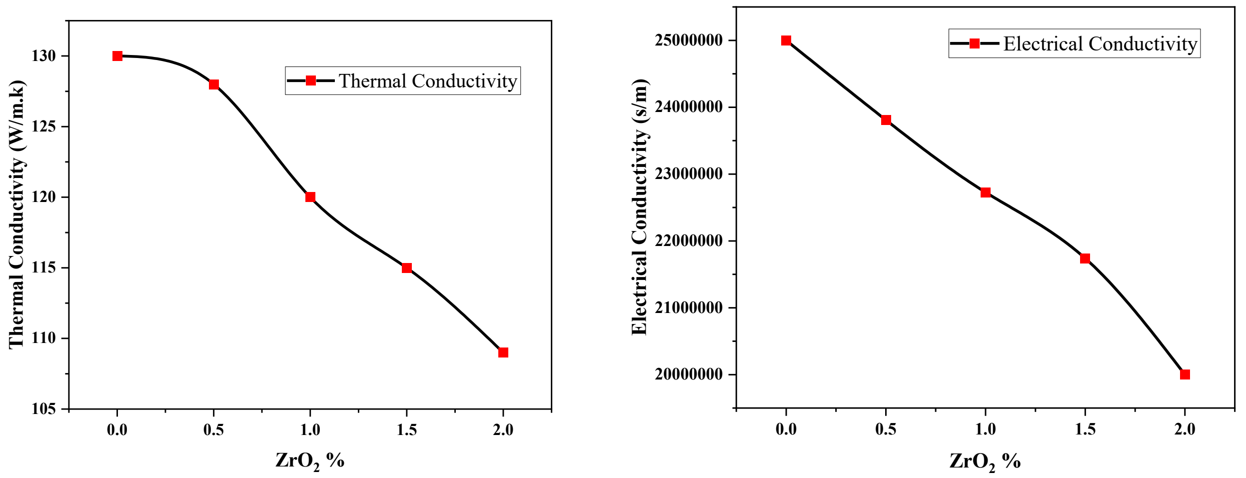

Figure 6(a, b): shows the effect of ZrO2 content on Thermal, Electrical conductivity for Al7075 Alloy.

Conclusions:

XRD and SEM analyses revealed a uniform distribution of ZrO_2 particles within the alloy, leading to an enhanced crystal structure and reduced defects. The addition of ZrO_2 increased density and reduced both apparent and true porosity due to improved inter-grain bonding and minimized voids. Electrical and thermal conductivities decreased with increasing ZrO_2 content, attributed to the insulating properties of ZrO_2 particles, which hinder electron and phonon transport. The results suggest the potential application of ZrO_2-reinforced 7075 aluminum alloys in fields requiring mechanical and structural enhancements, such as aerospace, automotive, and energy industries, considering the impact of reduced electrical and thermal conductivities.

References

[1] Sharma, J., et al. "Studies and scientific research analysis of aluminium (Al7075) metal matrix composite surface morphology." Materials Today: Proceedings (2023).

[2] Nagaral, Madeva, et al. "Characterization and tensile fractography of nano ZrO2 reinforced Copper-Zinc alloy composites." Frattura ed Integrità Strutturale 13.48 (2019): 370-376.

[3] Jawad, Saba I., and Mustafa H. Omar. "Experimental investigation on the influence of partially stabilised nano-ZrO2 on the properties of prepared clay-based refractory mortar." Journal of the Mechanical Behavior of Materials 32.1 (2022): 20220265.

[4] Sharma, J., et al. "Studies and scientific research analysis of aluminium (Al7075) metal matrix composite surface morphology." Materials Today: Proceedings (2023).

[5] Morampudi, Priyadarsini, et al. "Effect of nano ZrB2 particles on physical, mechanical and corrosion properties of Al6061 metal-matrix nano composites through stir casting route." Engineering Research Express 4.2 (2022): 025010.

[6] Abdulganiyu, Ibraheem Adekunle. THE INFLUENCE OF MICRO-FILLER ADDITION ON THE FLEXURAL AND IMPACT BEHAVIOR OF CARBON FIBER REINFORCED PHENOLIC. Diss. University of Saskatchewan, 2020.

[7] Montahaei, Reza, and H. R. Emamian. "The impact of micro-

wave-assisted sintering on fabrication of cobalt ferrite nanostructure foams for gas-sensing." Ceramics International 48.18 (2022): 26629-26637.

[8] Mahesha, C. R., et al. "[Retracted] Tribological Behavior of AA7075 Reinforced with Ag and ZrO2 Composites." Advances in Materials Science and Engineering 2022.1 (2022): 7105770.

[9] Meti VKV, Konaraddi R and Siddhalingeshwar IG. Mechanical and tribological properties of AA7075 based MMC processed through ultrasound-assisted casting technique. Mater Today Proc 2018; 5(11): 25677–25687.

[10] Umar, M. D., et al. "The influence of ZrO2 on tribological and mechanical characteristics of Al composite." Materials Today: Proceedings 115 (2024): 17-23.

[11] Azhar, Ahmad Zahirani Ahmad, et al. "The effect of dolomite addition onto the phases and hardness of zirconia toughened alumina." AIP Conference Proceedings. Vol. 2068. No. 1. AIP Publishing, 2019.

[12] Polayya, Chintada, C. S. P. Rao, and Veeresh Kumar GB. "Enhancing tribological and corrosion characteristics of AA2099/GNP metal matrix nanocomposites through parametric optimization using Taguchi Technique." Materials Research Express (2024).

[13] Polayya, Chintada, C. S. P. Rao, and Veeresh Kumar GB. "Enhancing tribological and corrosion characteristics of AA2099/GNP metal matrix nanocomposites through parametric optimization using Taguchi Technique." Materials Research Express (2024).

[14] Vemula, Ananda Mohan, U. Sudhakar, and K. Veera Raghavulu. "Mechanical and microstructural effects of SiN and ZrC reinforced AA7075 hybrid composite." Interactions 245.1 (2024): 302.

[15] Surani, Kapil, and Shailesh Patel. "Effect of powder mixed electrical discharge machining (PMEDM) on machining parameters of various materials with different powders: A review." Int. J. Res. Appl. Sci. Eng. Technol. 8 (2020): 614-630.